Photoelectrochemical Properties of Thin Films of Zinc Porphyrin Derivatives with Pyridyl Group

Kohshin TAKAHASHI,* Teruhisa KOMURA, and Hiroto IMANAGA
Department of Chemistry and Chemical Engineering, Faculty of Technology, Kanazawa University, Kodatsuno, Kanazawa 920
(Received August 8, 1988)

The cathodic photocurrents of the film electrodes of $ZnPyP_3P(3)$ and $ZnPyP_3P(4)$, ($PyP_3P(n)$, 5-(2-, 3-, and 4-pyridyl)-10,15,20-triphenylporphyrin, where (n) denotes the position of free bond of pyridyl group), were almost four times larger than that of ZnTPP (TPP, 5,10,15,20-tetraphenylporphyrin) in 0.01 mol dm^{-3} quinhydrone aqueous solution at pH 5. On the other hand, the very small anodic photocurrent was observed with the film electrodes of ZnTPyP(3) and ZnTPyP(4) (TPyP(n),5,10,15,20-tetra(2-, 3-, and 4-pyridyl)porphyrin). The photoelectrochemical properties of $ZnPyP_3P(2)$ and ZnTPyP(2) were distinct from those of other structural isomers, but approximately similar to those of ZnTPP. The conductivities of $ZnPyP_3P(n)$ films were about three oders of magnitude larger than those of ZnTPP and ZnTPyP(n) films. It was found from the absorption and resonance Raman spectra that the pyridyl group in porphyrin coordinated to zinc in another porphyrin in the solid films as well as in toluene and dichloromethane solutions. The molecular arrangement of zinc porphyrin in the solid film probably influenced the photoelectrochemical properties and the conductivity.

Much attention has been drawn to the photoelectrochemical properties of metalloporphyrin films from the standpoint of the conversion of solar to chemical and/or electrical energy.[1-8] The cathodic photocurrent is observed with the metalloporphyrin film electrode because of the formation of the blocking contact between a p-type semiconductor such as the metalloporphyrin film and an electrolytic solution.[1] The photocurrent quantum yield increases with a decrease in the first ring oxidation potential of metalloporphyrins,[2-5] and also with an increase in π-π interactions between neighbouring molecules.[5] On the other hand, the film of 5,10,15,20-tetra(3-pyridyl)porphyrin acts as an n-type semiconductor.[6]

In the present paper, the photoelectrochemical properties of zinc porphyrins as illustrated in Fig. 1 are investigated in a quinhydrone solution and compared with those of ZnTPP. We report that the pyridyl group in zinc porphyrins plays an important role in the photoelectrochemical behavior because of its coordination to zinc in another porphyrin.

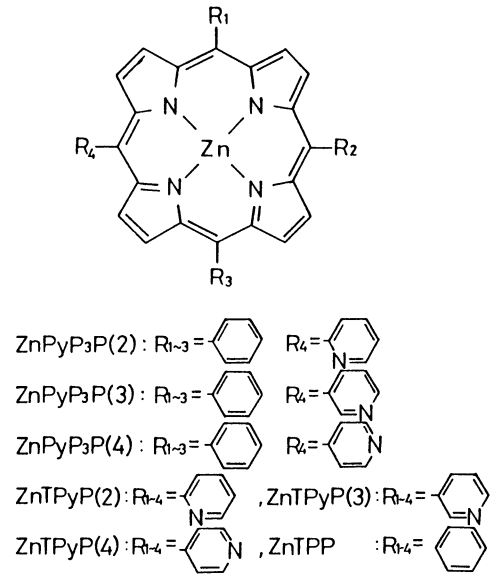

Fig. 1. Structures and abreviations of zinc porphyrins.

Experimental

H_2TPP, and $H_2PyP_3P(n)$ as well as $H_2TPyP(n)$ were synthesized and purified by the literature method.[9-11] Contamination with chlorine was oxidized by 2,3-dichloro-5,6-dicyano-*p*-benzoquinone.[12] ZnTPP and $ZnPyP_3P(n)$ as well as ZnTPyP(n) were synthesized by the literature method.[13] The products were purified by column chromatography on alumina. *p*-Benzoquinone was used after sublimation. Potassium chlorid and tetraethylammonium perchlorate (Et_4NClO_4) were used after double recrystallization from water. Toluene and dichloromethane were purified twice by distillation. *N,N*-Dimethylformamide (DMF) was twice distilled under reduced pressure in a N_2 atmosphere after dehydration by Molecular Sieves (4A 1/16) and barium oxide. Pyridine was twice distilled after dehydration by KOH. Other chemicals (reagent grade) were used without purification. All aqueous solutions were prepared with twice distilled water.

Absorption and second-derivative absorption spectra were taken on a Hitachi U-3210 spectrophotometer. The exciting radiation for resonance Raman spectra was provided by a Ar^+ laser (488 nm, Nippon Denki GSL3200). The scattering radiation was dispersed by a double monochromator (Jobin Yovon Ramanor HG2S), and detected by a cooled photomultiplier tube (Hamamatsu Photonics R464) and a photon-counter (Hamamatsu Photonics C1230). Porphyrin films were prepared on a Pt or glass plate by sublimation at pressure 4×10^{-3} Pa. Film electrodes were insulated from the electrolyte with epoxy resin except for the portion to be exposed to light (1 cm^2). A 500W xenon arc lamp (Ushio UXL-500D-O) was used as a white light source. The light was passed through a color filter (Toshiba L-39) and water (1 cm), and irradiated onto a film electrode in a N_2-purged solution thermostated at 25 °C. The light source for photo-

current action spectra measurements consisted of a 750 W halogen-tungsten lamp and a monochromator (Jasco CT-10). Monochromatic light intensity was measured with a chemical actinometer of $K[Cr(NH_3)_2(NCS)_4]$.[14] Photocurrent-voltage curves of the film electrodes were measured by using a potentiostat (Nikko Keisoku NPG-301), a potential sweeper (Nikko Keisoku NPG-2), and a three-electrode configuration. An X-Y plotter (Riken Denshi F-3B) was used to record current-voltage curves. A platinum wire (30 cm^2) was used as a counter electrode and a commercially available Ag/AgCl (in 3.33 M KCl aqueous solution, 1 M=1 mol dm^3) as the reference electrode. The conductivity of a surface-type cell of the solid film in vacuum was determined from a linear relationship between voltage and current. The measurements of current and voltage were performed by a picoammeter and a DC voltage source (Yokogawa Hewlet Packard 4140B). Cyclic voltammetry was performed in a N_2-purged solution by a Pt disk (diameter, 1 mm) as the working electrode, a Pt wire as the counter electrode, and Ag/0.01 M $AgNO_3$ in acetonitrile as the reference electrode. Half-wave potentials were measured with the scan rate of 100 mV s^{-1}, and as the average of cathodic and anodic peak potentials.

Results and Discussion

Dimerization of ($ZnPyP_3P(n)$) in Toluene and CH_2Cl_2. In nonbonding solvents such as toluene and CH_2Cl_2, $ZnPyP_3P(n)$ was slightly soluble and ZnTPyP(n) was insoluble, but in coordinating solvents such as DMF and pyridine, $ZnPyP_3P(n)$ and ZnTPyP(n) were soluble. The addition of pyridine to ZnTPP in toluene gave rise to a red shift of the absorption peak in the B and Q regions because of the formation of a monopyridine complex.[15] On the other hand, the absorption peak in the Q region of $ZnPyP_3P(2)$ in toluene was observed at a longer wavelength than that of ZnTPP in toluene, and the addition of pyridine gave rise to a blue shift of the Q band of $ZnPyP_3P(2)$. The Soret band of $ZnPyP_3P(2)$ in toluene and CH_2Cl_2 exhibited very broad spectra with very small molar extinction coefficients at the absorption peak (about 3×10^5 M^{-1} cm^{-1}) in comparison with those of other zinc porphyrins such as ZnTPP, $ZnPyP_3P(3)$ and $ZnPyP_3P(4)$, but in the solution containing pyridine, the sharp Soret band was observed with $ZnPyP_3P(2)$ as well as other zinc porphyrins. It was found from the second-derivative absorption spectra that the Soret band of $ZnPyP_3P(2)$ in CH_2Cl_2 consisted of two components and the peak wavelengths were 418 and 436 nm. The $Q_{1.0}$ bands of $ZnPyP_3P(n)$ in toluene and CH_2Cl_2 were broad. It was found from the second-derivative absorption spectra that the broad $Q_{1.0}$ bands consisted of two components and the peak wavelengths were near 550 and 565 nm. However, the absorption spectra in solution containing pyridine exhibited only one component near 560 nm. The absorption spectra of ZnTPP and $ZnPyP_3P(2)$ are shown in Fig. 2, and the absorption spectra features of zinc porphyrin derivatives are summarized in Table 1.

The absorption spectra of $ZnPyP_3P(n)$ in toluene distinctly changed in the range of 25 to 65 °C although that of ZnTPP hardly changed. Figure 3 shows the temperature-dependence of the absorption and second-

Table 1. Absorption Spectral Features of Zinc Porphyrins in Solutions at 25 °C and Solid Films at Room Temperature

Porphyrin	Media	$B_{0.0}$	$Q_{1.0}$	$Q_{0.0}$
		nm		
ZnTPP	CH_2Cl_2	419(59.5)[b]	548(2.16)	586(0.36)
	Toluene	424(48.8)	550(2.15)	589(0.34)
	1.2 M pyridine-toluene[a]	428(62.3)	562(2.01)	602(0.91)
	Film	435	553	590
$ZnPyP_3P(2)$	CH_2Cl_2	418(28.0)	566(1.63)	613(0.49)
	Toluene	424(29.4)	565(1.63)	612(0.43)
	1.2 M pyridine-toluene	428(57.9)	562(1.97)	602(0.74)
	Film	436	570	617
$ZnPyP_3P(3)$	CH_2Cl_2	420(44.6)	563(1.78)	605(0.73)
	Toluene	424(46.8)	561(1.49)	605(0.52)
	1.2 M pyridine-toluene	428(62.3)	563(2.02)	602(0.88)
	Film	445	570	610
$ZnPyP_3P(4)$	CH_2Cl_2	419(55.6)	558(1.50)	604(0.55)
	Toluene	423(49.5)	552(1.81)	600(0.34)
	1.2 M pyridine-toluene	428(63.1)	562(2.12)	602(0.84)
	Film	444	568	610
ZnTPyP(2)	1.2 M pyridine-CH_2Cl_2[c]	428	560	599
	Film	437	571	616
ZnTPyP(3)	1.2 M pyridine-CH_2Cl_2	429	563	601
	Film	446	570	610
ZnTPyP(4)	1.2 M pyridine-CH_2Cl_2	428	561	600
	Film	445	568	608

a) Toluene containing 1.2 M pyridine. b) The values in parentheses are molar extinction coefficients ($\varepsilon/10^4$ M^{-1} cm^{-1}). c) Dichloromethane containing 1.2 M pyridine.

derivative spectra in the Q region of $ZnPyP_3P(2)$ in toluene. The absorption spectra indicated two isobestic points at 530 and 557 nm. The minima of second-derivative absorption spectra corresponded to the absorption peaks, and thus two absorption peaks were present in the $Q_{1,0}$ region of the toluene solution at relatively high temperature. The absorbances of the absorption peaks at 568 and 613 nm decreased with an increase in temperature, while that at 551 nm increased.

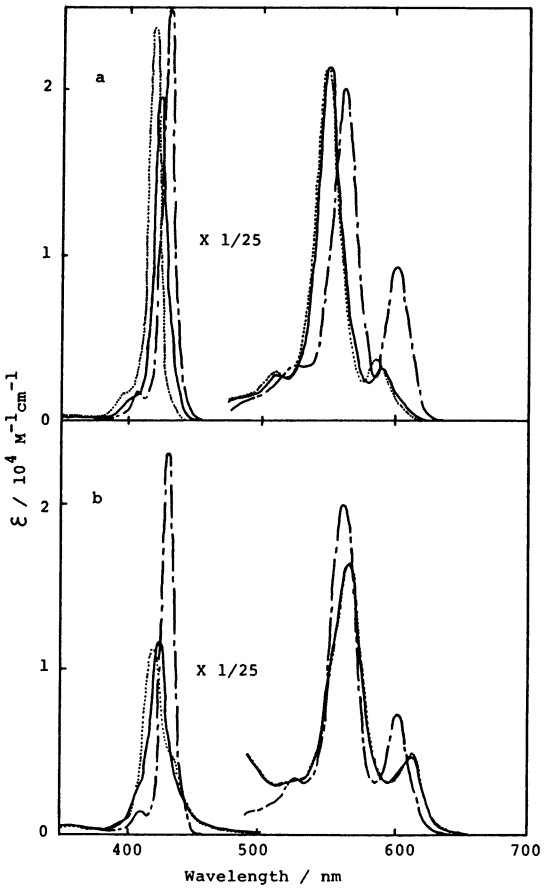

Fig. 2. Absorption spectra of ZnTPP(a) and $ZnPyP_3P(2)$(b) in toluene (——), CH_2Cl_2 (----), and toluene containing 1.2 M pyridine (-·--·-) at 25 °C.

The above results suggested that the pyridyl group in porphyrin coordinated to zinc in another porphyrin in nonbonding solvents such as toluene and CH_2Cl_2. However, the absorption spectra of $ZnPyP_3P(n)$ in toluene exhibited the temperature-dependence because the coordination bond between porphyrin molecules was relatively weak. Kirksey et al. demonstrated by means of ^1H NMR that the exchange between coordinated and uncoordinated pyridine was rapid in the solution of ZnTPP.[16] It was therefore presumed that the exchange between coordinated and uncoordinated $ZnPyP_3P(n)$ occurred in the toluene and CH_2Cl_2 solutions. Further, the dimer and monomer probably coexisted in the solution of $ZnPyP_3P(n)$ because the

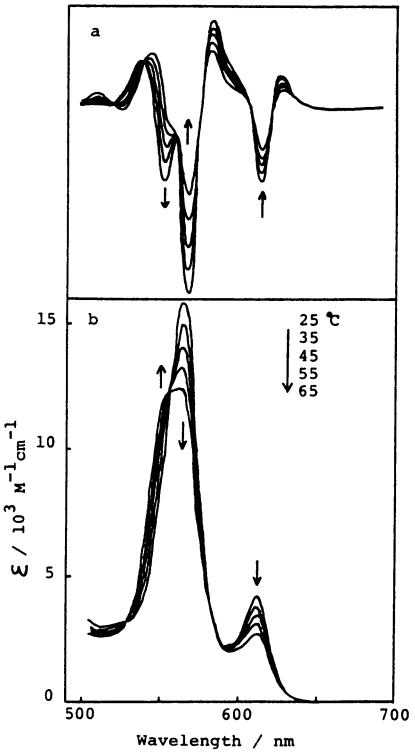

Fig. 3. Temperature-dependence of second-derivative(a) and absorption spectra(b) of $ZnPyP_3P(2)$ in toluene.

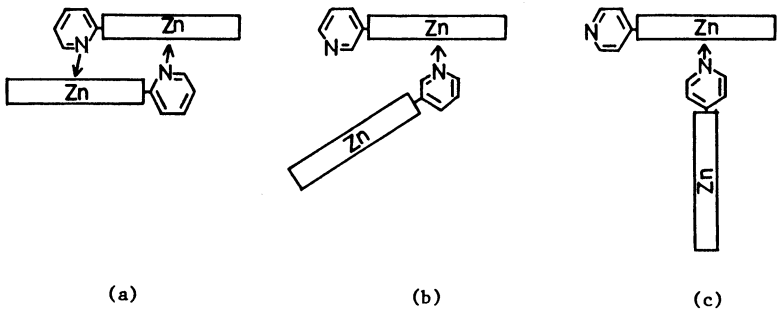

Fig. 4. Typical schematic dimer models of $ZnPyP_3P(2)$(a), $ZnPyP_3P(3)$(b) and $ZnPyP_3P(4)$(c).
▭ Denotes porphyrin ring, and N→Z coordination between Zn and N (pyridyl group).

absorption spectra at different temperatures passed through isobestic points. On the other hand, the Soret band of $ZnPyP_3P(2)$ in toluene and CH_2Cl_2 was especially broad in comparison with those of $ZnPyP_3P(3)$ and $ZnPyP_3P(4)$. Figure 4 shows typical schematic dimer models of $ZnPyP_3P(n)$. The π-π interaction between porphyrin rings in a dimer of $ZnPyP_3P(2)$ was probably large because only $ZnPyP_3P(2)$ can form a dimer of the face-to-face type. Therefore, the Soret band of $ZnPyP_3P(2)$ was broadened considerably.

The Photoelectrochemical Properties of Zinc Porphyrin Films. The photovoltaic effect was observed with the film electrodes of zinc porphyrin derivatives in a quinhydrone aqueous solution. Figure 5 shows the dependence of the short circuit photocurrent on the film thickness. The film electrodes of $ZnPyP_3P(3)$ and $ZnPyP_3P(4)$ exhibited the maximum cathodic photocurrent at the film thickness of 70 nm (about -12 $\mu A\ cm^{-2}$), and above 70 nm the photocurrent slightly decreased with an increase in film thickness. The film electrodes of $ZnPyP_3P(2)$, ZnTPyP(2), and ZnTPP exhibited the maximum cathodic photocurrent at the film thickness of 40—80 nm (-3—-8 $\mu A\,cm^{-2}$), and then the photocurrent suddenly decreased with an increase in film thickness. On the other hand, the film electrodes of ZnTPyP(3) and ZnTPyP(4) generated the very small anodic photocurrent (about 1 $\mu A\,cm^{-2}$). The dependence of the photocurrent of $ZnPyP_3P(2)$ and ZnTPyP(2) on the film thickness was distinct from that of other structural isomers, but approximately similar to that of ZnTPP. The film electrodes were consequently classified into three groups, (a) $ZnPyP_3P(3)$ and $ZnPyP_3P(4)$, (b) $ZnPyP_3P(2)$, ZnTPP, and ZnTPyP(2), (c) ZnTPyP(3) and ZnTPyP(4). The film electrode of each group indicated the different dependence of photocurrent on the film thickness because porphyrin of each group in the solid film may be oriented in different pattern. The molecular arrangement for porphyrin in the solid film will be discussed later. Figure 6 shows the photocurrent-voltage curves of the film electrodes of $ZnPyP_3P(4)$ and ZnTPyP(3) in 0.01 M quinone and hydroquinone solutions containing 0.2 M KCl at pH 5. The cathodic photocurrent was observed with $ZnPyP_3P(4)$ below the electrode potential of 0.5—0.6 V vs. AgCl/Ag in the quinone solution, and also the small anodic and cathodic photocurrents were observed in the hydroquinone solution because of the increase of conductivity of a zinc porphyrin film under irradiation. The onset potential of cathodic photocurrent in the quinone solution was larger than the reduction potential of quinone. The film electrodes of groups (a) and (b) indicated similar photocurrent-voltage curves to $ZnPyP_3P(4)$. These film electrodes consequently behaved as p-type semiconductors. The very thin film electrode of ZnTPyP(3) exhibited the anodic photocurrent above the electrode potential of -0.05 V vs. AgCl/Ag in the hydroquinone solution, and also the film electrode of ZnTPyP(4) (group (c)) indicated a similar photocurrent-voltage curve to ZnTPyP(3). Thus the film electrodes of group (c) exhibited different photocurrent-voltage curves from those of groups

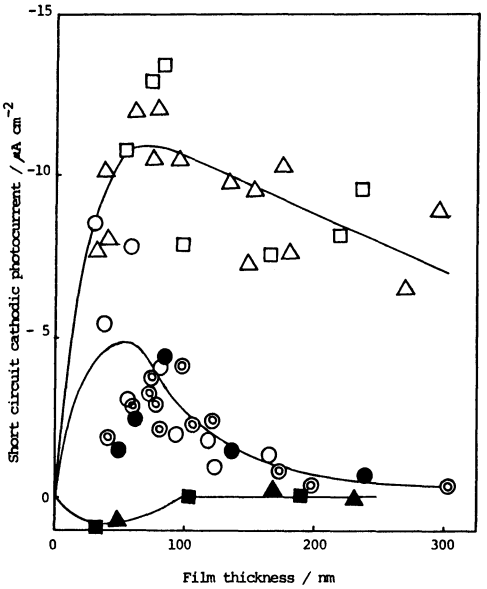

Fig. 5. Dependence of short circuit photocurrents of zinc porphyrins on film thickness in 0.01 M quinhydrone aqueous solution containing 0.2 M KCl at pH 5. A white light source was a 500 W xenon lamp.
◎: ZnTPP, ○: $ZnPyP_3P(2)$, □: $ZnPyP_3P(3)$, △: $ZnPyP_3P(4)$, ●: ZnTPyP(2), ■: ZnTPyP(3), ▲:, ZnTPyP(4).

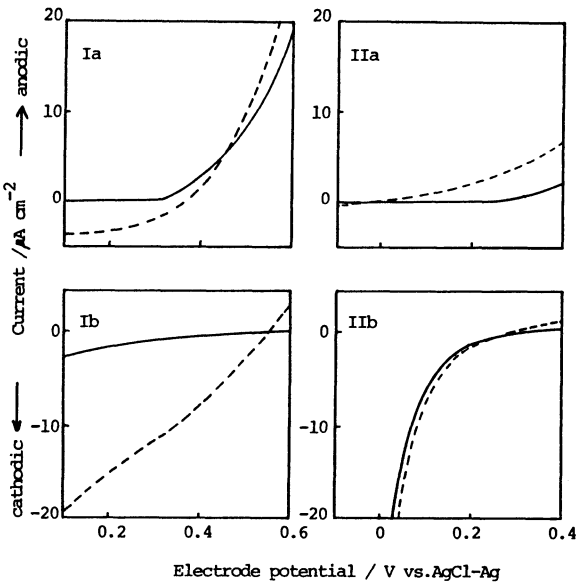

Fig. 6. Current-voltage curves of film electrodes of $ZnPyP_3P(4)$ (I, thickness 140 nm) and ZnTPyP(3) (II. thickness 30 nm) in 0.01 M hydroquinone(a) and quinone(b) aqueous solutions containing 0.2 M KCl at pH 5. A white light source was a 500 W xenon lamp.
——, in dark; ----, under irradiation.

(a) and (b). Figure 7 shows the short circuit photocurrent action spectrum of $ZnPyP_3P(4)$ film electrode in 0.01 M quinhydrone solution containing 0.2 M KCl at pH 5. The photocurrent was normalized in such a way that the incident light on the film electrode was constant (300 $\mu W\,cm^{-2}$). The photocurrent quantum yield of $ZnPyP_3P(4)$ was 0.16% at the irradiation wavelength of 440 nm. The action spectra were approximately the same as the absorption spectrum of the film. Therefore, the result suggested that the excited state of a zinc porphyrin molecule took part in the generation of the photocurrent.

The conductivities of $ZnPyP_3P(2)$, $ZnPyP_3P(3)$, and $ZnPyP_3P(4)$, which have only one pyridyl group in a molecule, were 8.3×10^{-11}, 6.6×10^{-10}, and 3.4×10^{-10} $S\,cm^{-1}$, respectively, and larger than that of ZnTPP (3×10^{-13} $S\,cm^{-1}$). On the other hand, the conductivities of ZnTPyP(n), which has four pyridyl groups in a molecule, were nearly equal to that of ZnTPP. The photoconductivity was observed with these films. The conductivities of zinc porphyrin films are summarized in Table 2. The pyridyl group in a porphyrin molecule was probably concerned with the molecular arrangement of porphyrin in the solid film because the conductivity was dependent on the number of the pyridyl group.

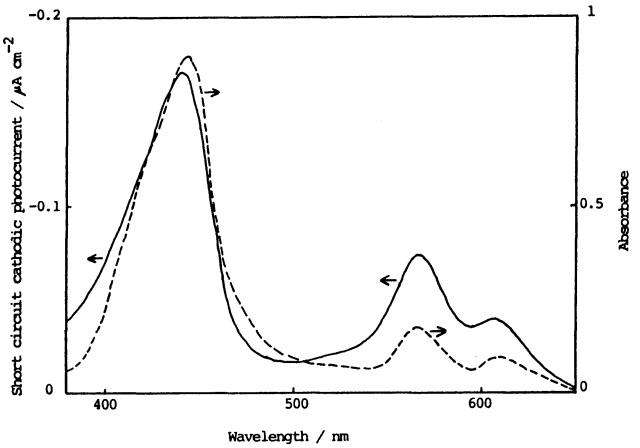

Fig. 7. Absorption(----) and photocurrent(——) action spectra of $ZnPyP_3P(4)$ film electrode (thickness 80 nm). An electrolytic solution was 0.01 M quinhydrone aqueous solution containing 0.2 MKCl at pH 5.

The photocurrent quantum yield of porphyrin film electrodes may be influenced by the following factors,[4] (i) the ease of charge carrier formation, (ii) packing of porphyrin molecules in the solid film, and (iii) the extent of π-π overlap between the porphyrin rings. The charge carrier may be easily formed with a decrease in the first ring oxidation potential of metalloporphyrins.[2-4] Table 3 summarizes the redox potentials of zinc porphyrin derivatives. ZnTPyP(n) was easily reduced but not oxidized in comparison with ZnTPP because of electron withdrawing of the pyridyl group in porphyrin. However, the redox potential of $ZnPyP_3P(n)$ was nearly equal to that of ZnTPP. Therefore, the difference of the photoelectrochemical properties of zinc porphyrin derivatives was not attributable to that of redox potentials. On the other hand, factors (ii) and (iii) presumably facilitated energy and electron transfers.[4]

The absorption peaks in the Q region of $ZnPyP_3P(n)$ and ZnTPyP(n) films were observed at longer wavelengths than that of a ZnTPP film (Table 1). The resonance Raman spectra were observed with zinc porphyrin films. We presumed that the signals in the range of 382 to 395 cm^{-1} were greatly ascribed to the stretching vibration of Zn-N (pyrole). The signals of $ZnPyP_3P(n)$ and ZnTPyP(n) were observed at lower wavenumbers than that of a ZnTPP film at 395 cm^{-1}

Table 2. Conductivities in the Dark (σ_d) and under Irradiation (σ_i)[a] of Zinc Porphyrin Films at Room Temperature

Porphyrin	σ_d/S cm^{-1}	σ_i/S cm^{-1}
ZnTPP	3×10^{-13}	9×10^{-12}
$ZnPyP_3P(2)$	8.3×10^{-11}	1.1×10^{-9}
$ZnPyP_3P(3)$	6.6×10^{-10}	5.3×10^{-9}
$ZnPyP_3P(4)$	3.4×10^{-10}	2.8×10^{-9}
ZnTPyP(2)	5×10^{-13}	1.5×10^{-11}
ZnTPyP(3)	8×10^{-13}	1.4×10^{-11}
ZnTPyP(4)	6×10^{-13}	4×10^{-12}

a) A white light source was a 500 W xenon lamp.

Table 3. Half-Wave Potentials of Zinc Porphyrins in DMF and Pyridine Solution Containing 0.1 M Et_4NClO_4 at Room Temperature

Porphyrin	Solvent	Reduction potential[a]/V		Oxidation potential[a]/V	
		2nd	1st	1st	2nd
ZnTPP	DMF	−2.15	−1.73	0.46	0.72[c]
$ZnPyP_3P(2)$	DMF	−2.14[b]	−1.71	0.50	0.75[c]
$ZnPyP_3P(3)$	DMF	−2.12	−1.68	0.54	0.77[c]
$ZnPyP_3(4)$	DMF	−2.08[b]	−1.67	0.53	0.79[c]
ZnTPyP(2)	Pyridine		−1.62	0.58[c]	
ZnTPyP(3)	Pyridine	−2.01[b]	−1.56	0.67[c]	
ZnTPyP(4)	Pyridine		−1.52	0.72[c]	

a) Measured against Ag/0.01 M $AgNO_3$ in acetonitrile. b) Cathodic-peak potential (irreversible reduction). c) Anodic-peak potential (irreversible oxidation).

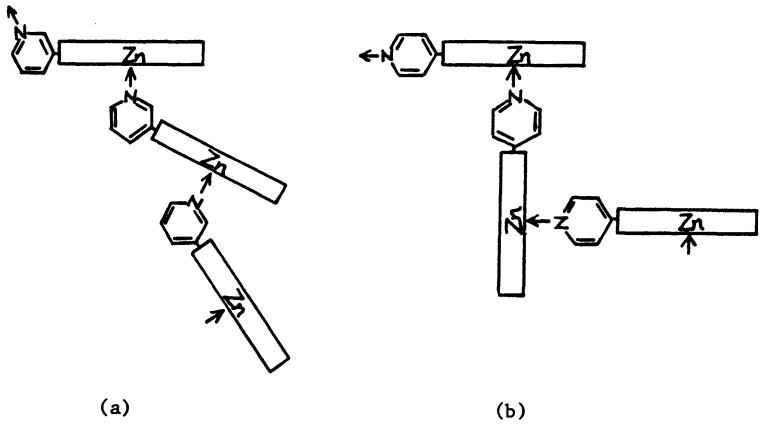

Fig. 8. Typical schematic models of molecular arrangement of $ZnPyP_3P(3)$ (a) and $ZnPyP_3P(4)$ (b) in a solid film.
□ Denotes porphyrin ring, and N→Z coordination between Zn and N (pyridyl group).

(difference, 8—13 cm^{-1}). The results suggested that the pyridyl group in porphyrin coordinated to zinc in another porphyrin in the solid film as well as in the toluene and CH_2Cl_2 solutions. $ZnPyP_3P(3)$ and $ZnPyP_3P(4)$ can form linear polymers as shown in Fig. 8 because the porphyrins have only one pyridyl group in a molecule, but ZnTPyP(3) and ZnTPyP(4) can form cross-linked polymers because of four pyridyl groups in a molecule. A linear polymer in porphyrin film facilitated the energy and electron transfers, but a cross-linked polymer interfered these transfers. On the other hand, $ZnPyP_3P(2)$ and ZnTPyP(2) can not form a polymer because of dimer formation of the face-to-face type (Fig. 4) and/or the steric hindrance by the porphyrin ring although a oligomer can be formed. Therefore, the absorption peaks in the Soret region of $ZnPyP_3P(2)$ and ZnTPyP(2) films were observed at shorter wavelengths than those of other structural isomer films, and at the same wavelength as that of ZnTPP film (Table 1). The film electrodes of $ZnPyP_3P(2)$ and ZnTPyP(2) consequently exhibited the same photoelectrochemical properties as a ZnTPP film electrode.

References

1) K. Yamashita, Y. Harima, and Y. Matsumura, *Bull. Chem. Soc. Jpn.*, **58**, 1761 (1985).
2) F. J. Kampas, K. Yamashita, and J. Fajer, *Nature*, **40**, 284 (1980).
3) T. Katsu, K. Tamagake, and Y. Fujita, *Chem. Lett.*, **1980**, 289.
4) K. Yamashita, *Chem. Lett.*, **1982**, 1085.
5) K. Yamashita, Y. Harima, H. Kubota, and H. Suzuki, *Bull. Chem. Soc. Jpn.*, **60**, 803 (1987).
6) K. Yamashita, Y. Matsumura, Y. Harima, S. Miura, and H. Suzuki, *Chem. Lett.*, **1984**, 489.
7) T. Kawai, K. Tanimura, and T. Sakata, *Chem. Phys. Lett.*, **56**, 541 (1978).
8) H. Jimbo, H. Yoneyama, and H. Tamura, *Photochem. Photobiol.*, **32**, 319 (1980).
9) A. D. Adler, F. R. Longo, J. D. Finarelli, J. Goldmacher, J. Assour, and L. Korsakoff, *J. Org. Chem.*, **32**, 476 (1967).
10) R. G. Little, J. A. Anton, P. A. Loach, and J. A. Ibers, *J. Heterocycl. Chem.*, **12**, 343 (1975).
11) K. Kalyanasundaram, *Inorg. Chem.*, **23**, 2453 (1984).
12) G. H. Barnett, M. F. Hadson, and K. M. Smith, *J. Chem. Soc., Perkin Trans. 1*, **1975**, 1401.
13) A. D. Adler, F. R. Longo, F. Kampas, and J. Kim, *J. Inorg. Nucl. Chem.*, **32**, 2443 (1970).
14) E. E. Wegner and A. W. Adamson, *J. Am. Chem. Soc.*, **88**, 394 (1966).
15) J. R. Miller and G. D. Dorough, *J. Am. Chem. Soc.*, **74**, 3977 (1952).
16) C. H. Kirksey, P. Hambright, and C. B. Storm, *Inorg. Chem.*, **8**, 2141 (1969).